

Terminal Settling Velocity and Drag Coefficient of Biofilm-Coated Particles at High Reynolds Numbers

Mehran Andalib, Jesse Zhu, and George Nakhla

Chemical and Biochemical Engineering Dept., The University of Western Ontario, London, ON, Canada N6A 5B8

DOI 10.1002/aic.12184

Published online January 20, 2010 in Wiley Online Library (wileyonlinelibrary.com).

The drag force (F_d) on bio-coated particles taken from two laboratory-scale liquid–solid circulating fluidized bed bioreactors (LSCFBBR) was studied. The terminal velocities (u_t) and Reynolds numbers (Re_t) of particles observed were higher than reported in the literature. Literature equations for determining u_t were found inadequate to predict drag coefficient (C_d) in $Re_t > 130$. A new equation for determining F_d as an explicit function of terminal settling velocity was generated based on Archimedes numbers (Ar) of the biofilm-coated particle. The proposed equation adequately predicted the terminal settling velocity of other literature data at lower Re_t of less than 130, with an accuracy >85%. © 2010 American Institute of Chemical Engineers AICHE J, 56: 2598–2606, 2010

Keywords: biofilm-coated particles, drag coefficient, terminal settling velocity, circulating fluidized bed bioreactor, Reynolds number, Archimedes number

Introduction

For the last 20 years, liquid–solid fluidized bed technology has been used for biological processes such as wastewater treatment. Because of the complexity of the hydrodynamic behavior, the design, and modeling of liquid–solid fluidized bed bioreactors (LSFBBR) are still being studied and there is still much to be discovered. In an LSFBBR, there are many processes that lead to the formation and attachment of biofilm to the carrier media. An increase in the thickness of the biofilm is a function of the attachment and growth rates while a decrease in its thickness depends on the decay and detachment rates. Changes in the biofilm thickness can vary the hydrodynamic behavior of fluidized beds significantly. Obviously the design of a fluidized bed bioreactors (FBBR) depends strongly on hydrodynamics such as the minimum fluidization velocity (u_{mf}), terminal settling velocity (u_t), bed expansion index, and particle effective density (ρ_p). Moreover, this technology has been used for different wastewater

treatment applications such as nitrification and denitrification which produce biofilm-coated particles with different physical characteristics.

There have been a few studies of drag coefficient (C_d) and u_t of biofilm-coated particles but predominantly for $Re_t \leq 100$. Primarily because such liquid–solid fluidized bioreactors need to operate at low liquid velocity which calls for small particle sizes. Biofilm particles are in the intermediate flow regime ($1 < Re_t < 100$) for the vast majority of cases when sand (0.5–1 mm) or similar material is used as an inert biofilm support.¹ With the new liquid–solid fluidized bed bioreactors developed by our group,² much higher liquid velocities and bigger particles can be used, thus providing the opportunity to study the flow properties of biofilm-coated particles as well as C_d and u_t at much higher Re_t .

Previous Works

Terminal settling velocity of biofilm covered particles

In general, when the velocity of a falling particle becomes constant, the summation of the F_d and buoyancy force (F_b)

Correspondence concerning this article should be addressed to M. Andalib at mandalib@uwo.ca

Table 1. Correlations for C_d for Biofilm Particles, Dry and Wet Biofilm Density

Reference	Re_t	Equation	C_d
5	50–100	(a)	$17.1 Re_t^{-0.47}$
6	40–90	(b)	$36.66 Re_t^{-0.67}$
7	15–87	(c)	$24 Re_t^{-1} + 21.55 Re_t^{-0.518}$
8	40–90	(d)	$24 Re_t^{-1} + 14.55 Re_t^{-0.48}$
10	7–90	(e)	$(0.8 + 6.1 Re_t^{-0.5})^2$
1	7–90	(f)	$29.6 Re_t^{-0.6}$
Reference	Equation	Dry biofilm density	
6	(g)	$\rho_d = 65 \text{ mg cm}^3 \text{ for } 0 < \delta \leq 300 \mu\text{m}$ $\rho_d = 98.6 - 0.106 \delta \text{ mg cm}^3 \text{ for } 300 < \delta \leq 630 \mu\text{m}$ $\rho_d = 30 \text{ mg cm}^3 \text{ for } \delta > 630 \mu\text{m}$	
11	(h)	$\begin{cases} \rho_d = 104.3 - 0.1245 \delta \text{ mg cm}^3 & \text{for } \delta \leq 620 \mu\text{m} \\ \rho_d = 26.9 \text{ mg cm}^3 & \text{for } \delta > 630 \mu\text{m} \end{cases}$	
12	(i)	$\begin{cases} \rho_d = 120(\delta/180)^{3.7} \text{ mg cm}^3 & \text{for } \delta \leq 180 \mu\text{m} \\ \rho_d = 120(\delta/180)^{-1.8} \text{ mg cm}^3 & \text{for } \delta > 180 \mu\text{m} \end{cases}$	
13	(j)	$\begin{cases} \rho_d = 191.4 - 0.224 \delta \text{ mg cm}^3 & \text{for } \delta \leq 593 \mu\text{m} \\ \rho_d = 58.6 \text{ mg cm}^3 & \text{for } \delta > 593 \mu\text{m} \end{cases}$	
14	(k)	$\rho_d = 0.43 \delta^{-0.26} \text{ mg cm}^3 \text{ for } 130 \leq \delta \leq 500 \mu\text{m}$	
Reference	Equation	Wet biofilm density (g cm^3)	
15	(l)	$\rho_w = 1.0$	
16	(m)	$\rho_w = 1.1$	
5	(n)	$\rho_w = 1.14$	
7	(o)	$\rho_w = 2.059 \rho_d + \rho_l$	
9	(q)	$\rho_w = \rho_d + \rho_l$	

equals the gravity force so that the solution of the dynamic-force balance results in Eq. (1).

$$u_t = \left[\frac{4gd_p(\rho_p - \rho_l)}{3C_d\rho_l} \right]^{0.5} \quad (1)$$

Based on nonlinear regression of experimental data, various researchers have proposed different C_d correlations at different Re_t . These correlations have been widely developed for smooth and rigid spherical particles and other conditions such as nonspherical porous particles.³ One of the most common in use and at the same time the simplest equations for smooth rigid spherical particles in the intermediate region, $0.3 < Re_t < 1000$, was suggested by Dallon and Christiansen (1968)⁴:

$$C_D = 18.5 Re_t^{-0.6} \quad (2)$$

Biofilm-coated particles are nearly spherical and Eq. (1) can be used to determine their u_t . However, they are neither smooth nor rigid and consequently the proposed C_d for smooth rigid particles could not be used. As a result, other equations relating C_d to Re_t , were developed for biofilm-coated particles by different researchers in predominantly two forms of (αRe_t^β) and $(24Re_t^{-1} + \alpha Re_t^\beta)$. All proposed equations had one thing in common: they are all functions of Re and consequently implicit in the terminal settling velocity. The suggested equations were defined in a certain

range of $Re_t < 100$ as mentioned in Table 1 Eqs. (a–f). So far, there has been no evidence showing the accuracy of these equations for a $Re_t > 100$.

Nicolella et al.¹⁰ argued that the ratio of C_d for biofilm particles to C_d for smooth and rigid solid particles is independent of biofilm thickness and concluded that particle deformability has a negligible effect on C_d . Although there is sufficient evidence in the literature that the drag coefficient for biofilm-coated particles is higher than rigid smooth particles, it has not been firmly proven that the surface roughness is the only dominant factor.

Unlike all previous suggested equations for drag coefficient as functions of Re_t , Karamanev¹⁷ suggested two equations for drag coefficient as functions of Archimedes number for spherical rigid particles and rising spheres.

Karamanev stated that the analysis of experimental data in the literature and correlations of the motion of falling particles shows that the best way to calculate the drag coefficient and the terminal velocity of particles in an infinite fluid is by describing the C_d as a function of Ar .

$$\text{where } Ar = \frac{gd_p^3(\rho_p - \rho_l)\rho_l}{\mu^2} \quad (3)$$

Karamanev's equations predicted all reliable existing data¹⁸ with the same accuracy as the equation suggested by Turton and Levenspiel.¹⁹ Furthermore, the correlations developed by Karamanev had the additional advantage of being explicit in terminal velocity.

Biofilm density

Considering the volumetric equivalent diameter for media to be d_m and volumetric equivalent diameter of biofilm-coated particles to be d_p , the effective density of bioparticles can be estimated using Eq. (4).

$$\rho_p = \left(\frac{d_m}{d_p}\right)^3 \rho_m + \left[1 - \left(\frac{d_m}{d_p}\right)^3\right] \rho_w \quad (4)$$

Biofilm thickness is defined as:

$$\delta = \frac{d_p - d_m}{2} \quad (5)$$

The biofilm dry density is defined as the mass of dry biomass VSS per unit wet biofilm volume. Various expressions for calculating biofilm dry density as a function of biofilm thickness have been summarized in Table 1 Eqs. (g–k).

Biofilm wet density can be defined as the density of the bulk of biofilm including the mass of dry biomass, the mass of interposing water within the biofilm structure and the water component of biocells. The direct measurement of the wet density of nonrigid, porous materials such as biofilm is extremely difficult.⁷ Various values suggested by different researchers for calculating biofilm wet density have been summarized in Table 1 Eqs. (l–q). None of those values was derived based on experimental data.

Materials and Methods

Two different laboratory-scale systems were used for biofilm sampling. As shown in Figure 1, the patented circulating fluidized bed bioreactor (CFBBR, US patent no 7,261,811 B2) consists of an anoxic plexi-glass column as a riser and an aerobic plexi-glass column as a downer. The riser and downer inner diameters were 2 and 7.6 cm, respectively and heights were 3 and 2.5 m, respectively. The synthetic wastewater flow rate to the system was 48 l day⁻¹ with the average organic loading of 2.9 kg COD m⁻³ day⁻¹ and the average nitrogen loading of 0.33 kg N m⁻³ day⁻¹. The system was running with a superficial liquid velocity of $u_s = 1.4$ – 2.0 cm s⁻¹ in the riser and $u_s = 0.26$ cm s⁻¹ in the downer. The second system in use was a twin fluidized bed bioreactor (TFBBR) with particle recirculation. The two columns were both 4 m high. Each rectangular area of plexi-glass column was 8.9 cm by 5 cm. The feed flow rate was 180–220 l day⁻¹ with the average organic loading of 1.5–1.88 kg COD m⁻³ day⁻¹ and the average nitrogen loading of 0.18–0.22 kg N m⁻³ day⁻¹. The system was running with $u_s = 0.54$ cm s⁻¹ in the aerobic column and a superficial liquid velocity of $u_s = 0.37$ – 0.64 cm s⁻¹ in the anoxic column. The carrier media used in both systems was lava rock ranging in size from 400 to 2000 μ m with a true density of 2.63 g cm⁻³ and porosity of 0.62. In the TFBBR particle recirculation, was accomplished through a positive displacement particle transfer pump between the twin columns, while in the CFBBR biofilm-coated particles were transferred naturally from the anoxic column to the aerobic column due to a decrease in particle density as a result of biofilm development and consequently reaching the terminal settling velocity.

Synthetic feed was used for both systems, which was prepared using tap water in addition to other chemicals. The chemical oxygen demand (sCOD) of the feed was 250 ± 10 mg l⁻¹ as a result of dissolving 31.25 g of sodium acetate in 100 l of deionized water and a concentration of 25 ± 2 mg l⁻¹ NH₃-N as a result of adding 5 g of NH₄Cl to the 100 l of deionized water. A concentration of 3 ± 0.5 mg l⁻¹ PO₄-P and nutrients were also provided.

Biofilm-coated particles were periodically taken from sampling ports along the columns for the purpose of measuring the biofilm dry and wet densities as well as the terminal settling velocity over a period of 3 months. The sampling took place by a syringe at the same pressure inside each column to minimize disturbances to the biofilm structure. Each particle was then transferred to a small container filled with water. Using a microscope MITUTOYO, Sakada, Japan with magnification 50 \times coupled with a camera LEICA DC300, Germany, each particle was photographed and then transferred to its container. The volumetric equivalent particle diameter (d_p) and the volumetric equivalent media diameter (d_m) were measured with the VISIONGAUGE software (Flexbar Machine, New York) synchronized to the camera. To maximize the accuracy of the measurements, all the measurements were periodically checked with the microscope's Standard Measurement Ruler. Figure 1 also shows some estimated measurements of biofilm and media diameters.

To measure u_t experimentally, biofilm-coated particles were sequentially transferred to a third column 6 m high, 32 cm in diameter, thus nullifying the wall effects due to $d_c \gg 50 d_p$. Clean water was used to fill this column. After letting the particles reach their constant settling velocity (3 m below the top of the column), the travel time between two fixed points (50 cm) was measured. Falling particles with nonstraight paths and nonparallel to the centerline were neglected. Nonspherical particles were also neglected.

To measure biofilm dry density, Eq. (6) was used.²⁰ Samples were taken and photographed to measure d_p and d_c and then sonicated (Aquasonic SK 1200H Kupos, China) for 3 h at 30°C to remove the biofilm from the media. As the biofilm sizes were not completely identical in each sample, average values for diameters were considered. Each sampling took place at a different stage of biofilm development and also hydrodynamic conditions such as superficial liquid velocity. As a result, different biofilm thicknesses were obtained at different times but the thicknesses of the biofilms were relatively equal in each sampling.

$$\rho_d = \frac{X\rho_m}{\gamma^3 - 1} \quad (6)$$

As all proposed equations for the wet biofilm density are based on theories without any verification by experimental data, a hydrostatic method was developed to measure the wet biofilm density accurately. The experimental data verified the most accurate equation to calculate this value. Samples were taken, photographed for measuring the biofilm thickness and then sonicated to remove the biofilm from the media. Different concentrations of sodium acetate were dissolved in deionized water in order to make liquids with different densities of 1060, 1065, 1070, 1075, 1080, 1085,

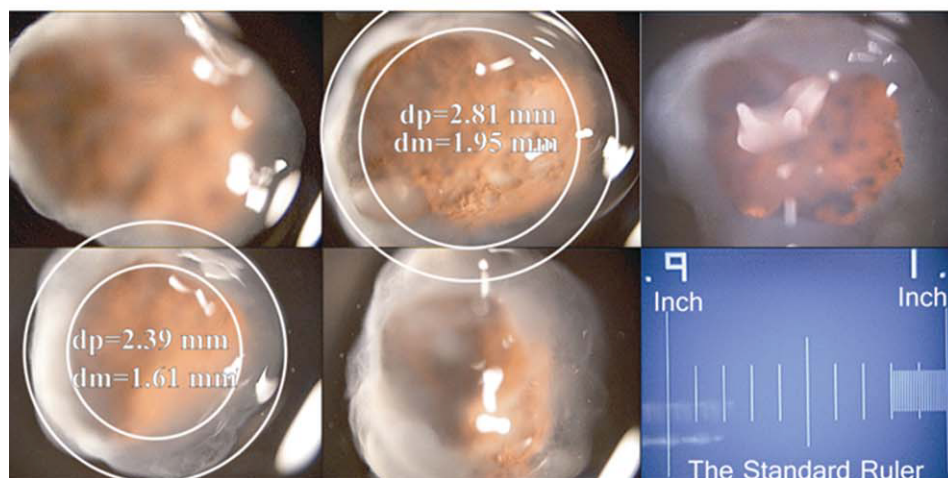
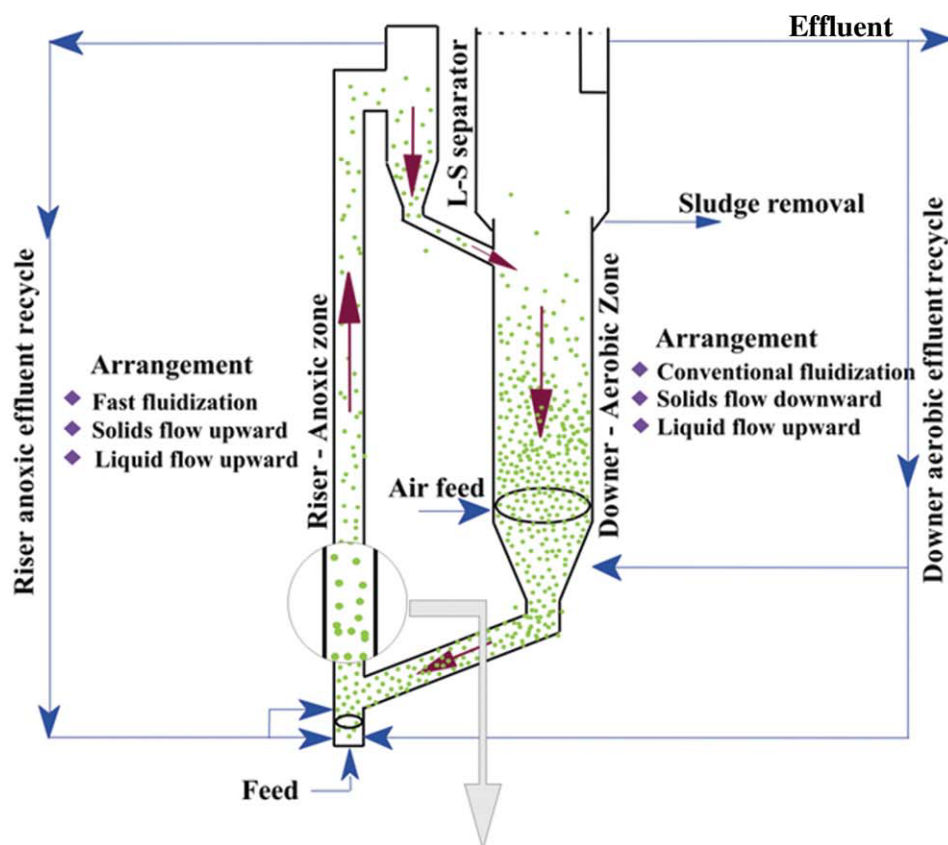


Figure 1. Schematic of a liquid–solid circulating fluidized bed used for the experiments and the microscopic pictures of biofilm particles and measurements of biofilm and media diameters.

[Color figure can be viewed in the online issue, which is available at wileyonlinelibrary.com.]

1090, and 1095 kg m⁻³. The density of liquid in each vial was measured and verified by hydrometers. Eight 100-ml glass cylinders were filled with the provided liquids. The biofilm without carrier media was placed inside the vials and then well shaken to lessen the size of bioparticles in order to uniform the effect of buoyancy force. After 2 h bio-particles in one vial did neither float nor settle. As the gravity force equaled to the buoyancy force, the density of bioparticles,

wet density, was considered equal to the density of the liquid.

Results and Discussion

Figure 2 presents the measured results of dry and wet biofilm densities, along with correlations proposed by different researchers. The experimental dry biofilm density data from

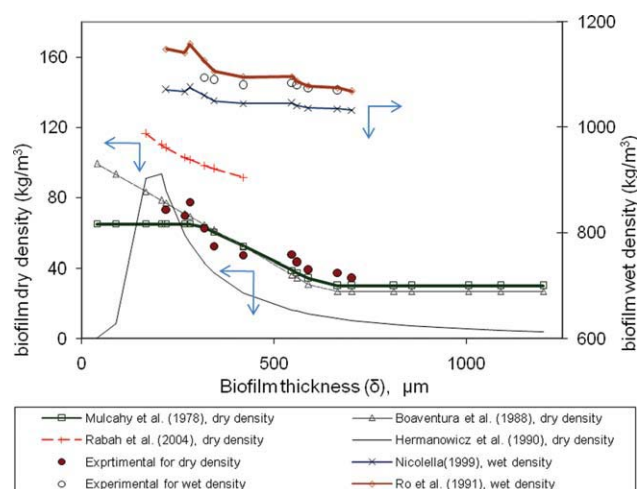


Figure 2. Comparison of experimental results of dry and wet densities of attached biofilm with different thickness with that predicted by existing correlations.

[Color figure can be viewed in the online issue, which is available at wileyonlinelibrary.com.]

this work fit two equations proposed by Boaventura et al.¹¹ and Mulcahy et al.⁶, Table 1 Eqs. (h and g) respectively, with an overall accuracy of 89% and 93%. Despite the lower accuracy of prediction of dry biofilm density, Boaventura's equation was used in this work to be consistent with Nicolella's study where the same equation was used.

On the other hand, the experimental data of wet biofilm density had a better correlation with the equation proposed by Ro et al.⁷ which was therefore used to estimate the biofilm wet density. It is interesting to note that the proposed equations for dry biofilm density were predominantly based on their experimental data while equations for wet biofilm density were predominantly theoretical due to a lack of a standard experimental method. In this study however the experimental method, described earlier, was developed to measure the wet biofilm density.

The terminal settling velocity tests discussed in this paper were conducted over a period of 3 months and were based on one hundred data of biofilm-coated particles. To summarize the experimental data, results from 20 randomly selected experiments of the 100 are shown in Table 2. As only the relatively spherical particles were counted in this experiment, Eq. (1) was used to estimate the value of experimental drag

coefficient C_d . In addition, Eq. (7) was used to estimate the experimental Re_t based on observations of the terminal velocity and particle diameter.

$$Re_t = \frac{\rho_l u_t d_p}{\mu_l} \quad (7)$$

From the above equation, the experimental Re_t was found to be in the range of 148–281. Figure 3 shows a comparison between all of the proposed equations (as given in Table 1) for the C_d of biofilm-coated particles and the experimental data from this work. It is apparent from Figure 3 that the proposed equations for $7 < Re_t < 100$ fail to predict the drag coefficients at $Re_t > 130$. Figure 3 also compares the experimental data generated by Nicolella et al.¹⁰ with his suggested equation. The graph shows that at some Re_t , shown by the arrows, there is a deviation of more than thirty percent between his experimental C_d and the predicted C_d from his equation which denies a mono-dependency of drag coefficient on Reynolds number in biofilm-coated particles. It is worth mentioning that even at the range of $7 < Re_t < 100$, the deviation between the experimental C_d at the same Re_t exceeded 200%.

To explain why the bioparticle Re_t in this work is much higher than the previous works, Figure 4 was produced. In this figure, the values of bioparticle diameters, biofilm thicknesses and bioparticle effective densities of all the existing experimental data were compared. The graph shows that the equivalent diameters of the bioparticles in this experiment, 2.3–3.3 mm, were higher than the particle diameters presented in previous works, 0.4–2.6 mm,¹⁰ 0.7–1.2 mm,⁵ and 0.8–1.5 mm.²¹ At certain points, there are similar particle diameters to other data even though the values of density at those points were much lower due to the higher biofilm thickness. As Re_t is a function of diameter $Re_t \propto d_p$ and terminal velocity, and the terminal velocity is a function of body force $u_t \propto \rho_p^{0.5}$, a higher value of Reynolds numbers in this work is logically expected.

Figure 5a represents a comparison between the predicted u_t using C_d proposed by Nicolella¹⁰ and the experimental data existing so far in the literature from five other researchers. The graph shows an acceptable result within 15% average error for data with $Re_t < 100$. However, when Re_t is above 130, data from this work, there is a significant increased deviation between the experimental data and calculated values.

Table 2. Some Terminal-Settling Velocities Out of Over One Hundred Measurement Data

d_m (mm)	d_p (mm)	ρ_p (kg m ⁻³)	u_t (mm s ⁻¹)	Re_t	d_m (mm)	d_p (mm)	ρ_p (kg m ⁻³)	u_t (mm s ⁻¹)	Re_t
1.91	2.81	1587.3	83.6	235	1.62	2.39	1598.8	88.3	211
1.71	2.52	1595.3	75.7	191	1.67	2.47	1596.8	73.1	180.5
1.57	2.31	1601.0	87.7	202.5	1.91	2.53	1787.0	73.6	186
1.71	2.82	1425.6	68.1	192	1.82	2.57	1664.4	66.6	171
1.92	2.95	1510.6	71.4	210.6	1.55	2.29	1590.8	80.4	185
1.61	2.51	1512.7	71.9	180.5	1.41	2.32	1443.6	71.5	166
1.70	2.51	1595.2	63.6	160	1.51	2.43	1466.7	70.3	171
1.75	2.63	1556.9	79.0	208	1.65	2.33	1666.7	66.0	154
2.09	2.68	1855.1	74.4	199.5	2.04	3.00	1592.0	67.0	201
2.01	3.09	1579.6	87.7	271	2.02	3.34	1575.5	85.8	286.5

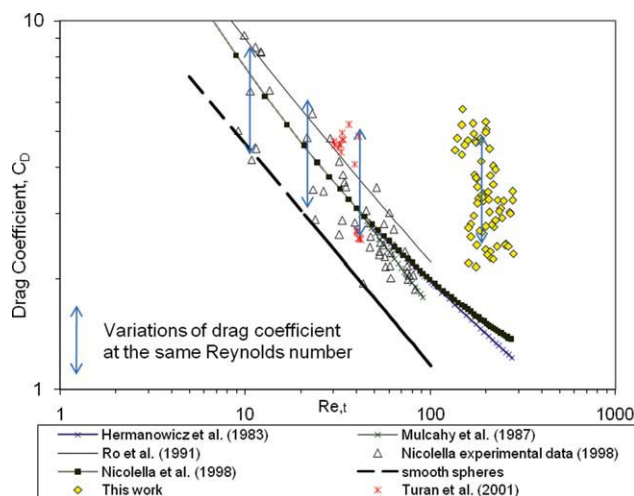


Figure 3. Comparison of experimental drag coefficient and that predicted with existing equations for biofilm-coated particles.

[Color figure can be viewed in the online issue, which is available at wileyonlinelibrary.com.]

To check further the suitability of the literature correlations for predicting terminal settling velocity at higher velocities, the following correlations were derived. As mentioned earlier, most equations for drag coefficient of biofilm are written as αRe_t^β , shown Table 1, so we can rewrite this definition as

$$C_d = \alpha \left(\frac{d_p u_t \rho_l}{\mu_l} \right)^\beta = \left[\alpha^{1/\beta} \cdot \frac{\rho_l}{\mu_l} \right]^\beta \cdot (u_t \cdot d_p)^\beta \quad (8)$$

Combining Eq. (8) with Eq. (1) results:

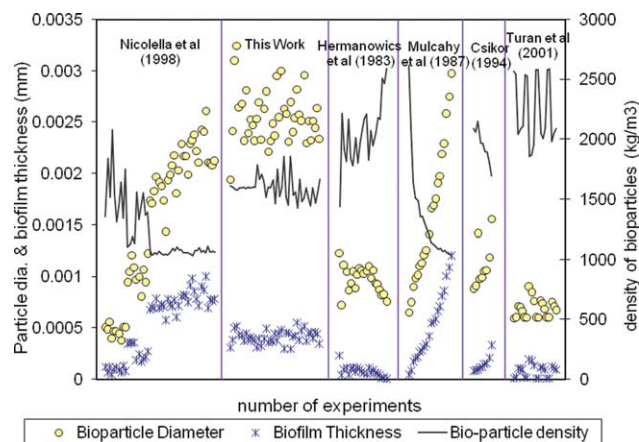
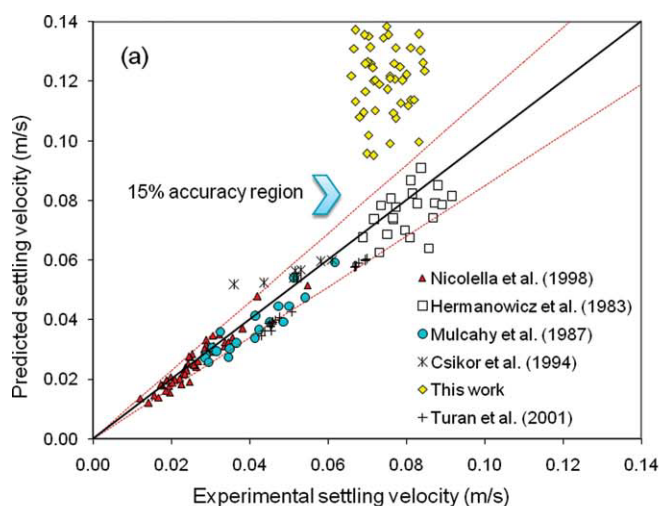


Figure 4. Comparison of diameter, thickness and the effective density of the biofilm-coated particles from experiments.

[Color figure can be viewed in the online issue, which is available at wileyonlinelibrary.com.]

$$u_t = \left[\frac{4g\mu_l^\beta}{3\alpha\rho_l^{\beta+1}} \right]^{1/2+\beta} \cdot (\rho_p - \rho_l)^{1/2+\beta} \cdot d_p^{1-\beta/2+\beta} \quad (9)$$

Assuming the same liquid characteristics, according to Eq. (9), terminal settling velocity is a function of $(\rho_p - \rho_l)^{1/2+\beta}$ and $d_p^{1-\beta/2+\beta}$ so the order of change of terminal velocity between two particles (1) and (2) should be:

$$\frac{u_{t,2}}{u_{t,1}} = \left(\frac{\rho_{p,2} - \rho_l}{\rho_{p,1} - \rho_l} \right)^{1/2+\beta} \left(\frac{d_{p,2}}{d_{p,1}} \right)^{1-\beta/2+\beta} \quad (10)$$

According to Nicolella et al.¹ β equals to -0.6 . Figure 5b shows the values of $\frac{u_{t,i}}{u_{t,1}}$ calculated by Eq. (10) for 50

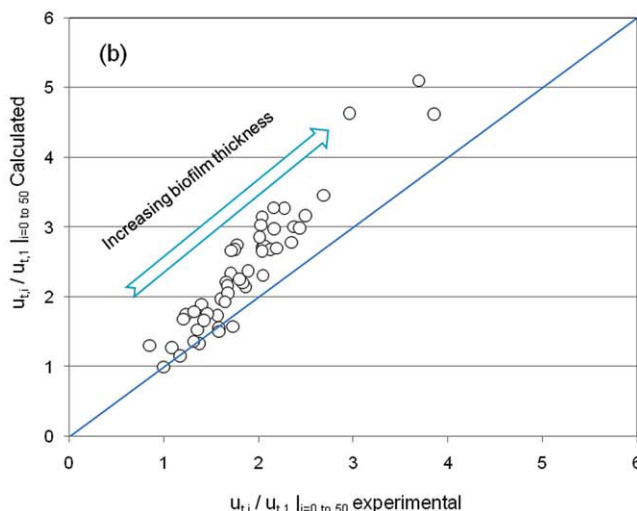


Figure 5. (a) Comparison of experimental terminal velocities and the predicted terminal velocities using Nicolella's equation, $C_d = f(Re)$. (b) Comparison of calculated the ratio by Eq. (9) versus experimental ratio.

[Color figure can be viewed in the online issue, which is available at wileyonlinelibrary.com.]

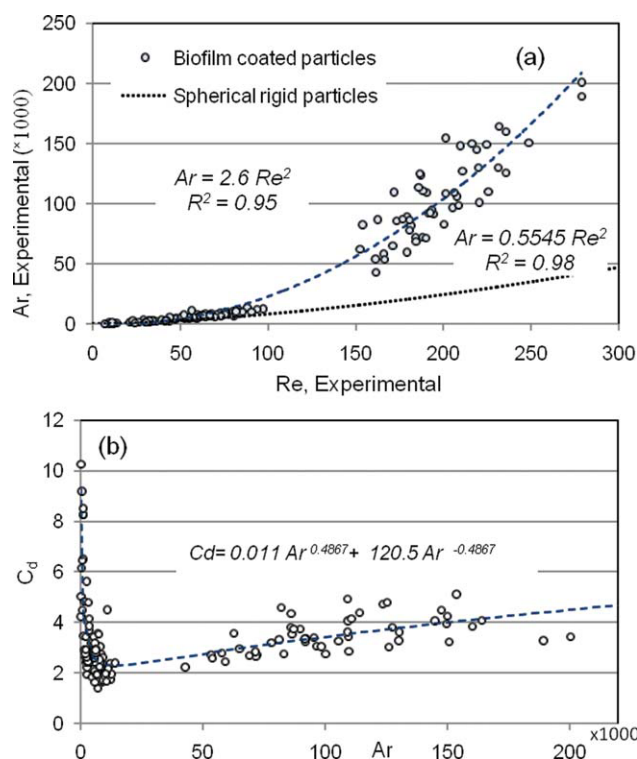


Figure 6. (a) Archimedes number as a function of Reynolds number for experimental data of biofilm-coated particles (b) Drag coefficient as a function of Archimedes number for experimental data of biofilm-coated particles.

[Color figure can be viewed in the online issue, which is available at wileyonlinelibrary.com.]

data reported¹⁰ versus the experimental values of $\frac{u_{t,i}}{u_{t,1}}$ for $i=1-50$ for the same reported data. The figure demonstrates that the terminal settling velocity calculated by proposed equation¹⁰ has a good agreement with the experimental values at lower settling velocities whereas the accuracy of the predicted terminal settling velocity decreases when the biofilm settling velocity and consequently Re_t increases.

Equation (1) can also be written in the dimensionless form of Eq. (11):

$$Re_t^2 = \frac{4 Ar}{3 C_d} \quad (11)$$

Equation (11) represents an analytical relationship between three dimensionless parameters of particle settling motion: the Reynolds number, the Archimedes number and the drag coefficient. Based on this equation, the drag coefficient of particles has a linear dependency with the multiplication of their $Ar \cdot Re_t^{-2}$. According to Eq. (11) a two-dimensional plot between any two of these three variables can be depicted.²²

To study the experimental relationships between the three mentioned dimensionless parameters of particle motions, Archimedes numbers for experimental data of biofilm-coated particles were drawn versus the experimental Re_t in

Figure 6a. The Archimedes number for each particle was calculated based on Eq. (3). The best fitted curve in the format of Eq. (11) was as follows:

$$Ar = 2.6 Re_t^2 \quad \text{for } 310 < Ar < 2.5 \times 10^5$$

$$\text{and } 7 < Re_t < 300 \quad (12)$$

Figure 6a shows that biofilm-coated particles have the Archimedes values of less than 32,508 in the Reynolds range of less than 97. In this range of Re_t , a smaller fluctuation in the Archimedes values was observed. It can also be seen that the Archimedes number increasing rate with increasing Re_t in biofilm-coated particles is higher than the spherical rigid particles.

The same concept was applied for the drag coefficient and the Archimedes number and the result is shown in Figure 6b, which indicates that the maximum drag coefficient of 9–10 occurs when the Ar is in the range of 500–1000 and Re_t is less than 25, also there is a significant decrease in the value of C_d while the Ar increases to 15,000 and Re_t to 100. At higher values of Ar and Re_t , the drag coefficient seems to become constant at the value of 4. Karamanev²² also reported a trend for rising particles similar to what was observed for biofilm-coated particles where there was a significant decrease in the value of C_d until Ar of 15,000 and after that C_d levels out to 0.95. In addition, a comparison between the Figures 6b and 3 shows that the trend of drag coefficient versus Archimedes number is much more consistent and reliable than the drag coefficient versus Reynolds number. Equation (13) was found an acceptable fitted curve on the existing biofilm particles experimental data that relates directly the value of the drag coefficient to the Archimedes number.

$$C_d = a Ar^b + c Ar^{-b} \quad \text{where } \begin{cases} a = 0.011 \\ b = 0.487 \\ c = 120.5 \end{cases} \quad (13)$$

Using this equation along with Eq. (1), the terminal settling velocities were calculated implicitly for each particle

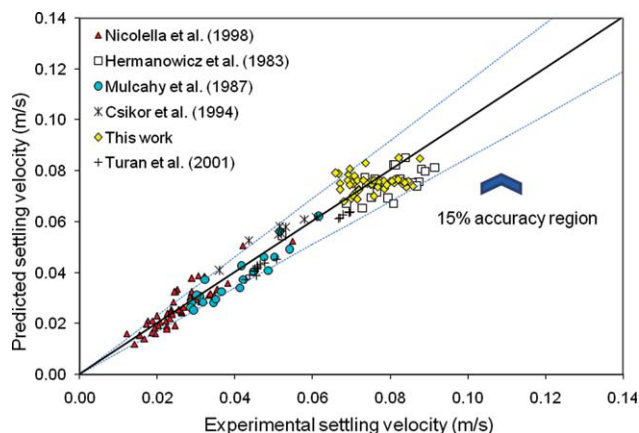


Figure 7. Comparison of experimental data for terminal velocity of biofilm-coated particles with the proposed equation, $C_d = f(Ar)$, Eq. (13).

[Color figure can be viewed in the online issue, which is available at wileyonlinelibrary.com.]

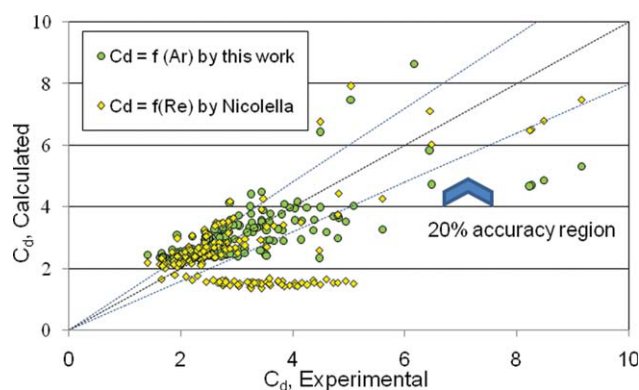


Figure 8. Comparison between the predicted values of drag coefficient for biofilm-coated particles by this work and Nicolella et al.⁹ with the experimental data existing in the literature.

[Color figure can be viewed in the online issue, which is available at wileyonlinelibrary.com.]

and depicted versus the terminal velocity experimental data in Figure 7. In this figure, it can be clearly seen that the calculated terminal velocities closely match the experimental data from different researchers. Compared to all experimental data, this equation predicted the terminal velocities with average errors $5.9 \pm 4.6\%$, $11.1 \pm 8.4\%$, $9.5 \pm 6.5\%$, $7.6 \pm 5.3\%$, $8.8 \pm 4.8\%$, and $10.8 \pm 2.5\%$ for this work, Nicolella,¹⁰ Mulcahy,⁶ Hermaniwicz,⁵ Csikor,²¹ and Turan,²³ respectively. To compare, equation suggested by Nicolella¹⁰, as the most previously reliable equation for biofilm particles, predict the terminal velocities with errors of $37.9 \pm 7.6\%$, $8.45 \pm 6.6\%$, $11.2 \pm 7.6\%$, $9.4 \pm 9.6\%$, $9.4 \pm 9.5\%$, and $18.1 \pm 2.8\%$ for this work, Nicolella,¹⁰ Mulcahy,⁶ Hermaniwicz,⁵ Csikor,²¹ and Turan,²² respectively. The above data clearly shows a better prediction of terminal velocity by equation suggested based on Archimedes than the other. Considering the margin of error in experimental data in addition to a lack of standard method for measuring some biofilm particle characteristics, the above equation gives an accurate prediction of drag coefficient in a wide range of $7 < Re_t < 300$ and $310 < Ar < 2.5 \times 10^5$ for biofilm particle motion.

To elaborate on the values of drag coefficient predicted by this work as a function of Archimedes number and work done by Nicolella¹⁰ as a function of Reynolds, Figure 8 was generated. The figure shows a much better agreement between the calculated values by this work and experimental data than equation proposed by Nicolella.¹⁰

It is clear that the value of C_d for biofilm-coated particles is higher than smooth spherical particles and different researchers generated equations based on the theoretical assumption of a higher roughness of bioparticle surfaces and deformability. However, no further explanation was found to explain the higher drag force of larger biofilm covered particles than what predicted previously.

Conclusions

Based on experiment, the proposed equations by Ro⁷ and Mulcahy⁶ to determine the wet and dry biofilm densities respectively were found the most suitable among the litera-

ture equations. A terminal velocity test for biofilm-coated particles was conducted. The Reynolds numbers related to terminal velocity were higher than the literature data due to bigger particle sizes. The literature equations were not adequate for $Re_t > 130$. A new explanation of drag coefficient for a wide range of Re_t and based on a biofilm-coated particle Archimedes number, a new equation was generated that was able to predict terminal settling velocity with average error of $5.9 \pm 4.6\%$, $11.1 \pm 8.4\%$, $9.5 \pm 6.5\%$, $7.6 \pm 5.3\%$, $8.8 \pm 4.8\%$, and $10.8 \pm 2.5\%$ for this work, Nicolella,¹⁰ Mulcahy,⁶ Hermaniwicz,⁵ Csikor,²¹ and Turan,²³ respectively. This equation is explicit in terminal settling velocity and is valid within $310 < Ar < 2.5 \times 10^5$ and $7 < Re_t < 300$.

Notation

Ar = Archimedes number
 d_c = the diameter of column (L)
 d_m = the volumetric equivalent diameter of the media (L)
 d_p = the volumetric equivalent diameter of the biofilm-coated particles (L)
 C_d = drag coefficient for an isolated particle
 F_b = buoyant force ($M L S^{-2}$)
 F_d = drag force on an isolated particle ($M L S^{-2}$)
 g = gravitational constant ($L S^{-2}$)
 m, n = constant coefficients
 Re_t = Reynolds number at terminal settling velocity
 u = relative velocity of fluid and particle ($L S^{-1}$)
 u_s = superficial liquid velocity in a fluidized bed ($L S^{-1}$)
 u_t = terminal settling velocity ($L S^{-1}$)
 V_p = particle volume (L^3)
 \bar{X} = dry mass of biofilm/media diameter (mg VSS/g media)

Greek letters

α, β = constant coefficients
 ε = voidage
 δ = biofilm thickness (L)
 γ = bio-particle diameter/media diameter = d_p/d_m
 μ_l = liquid dynamic viscosity ($M L^{-1} S^{-1}$)
 ρ_a = true dry density of bacteria ($M L^{-3}$)
 ρ_B = fluidized bed suspension density ($M L^{-3}$)
 ρ_m = true density of media ($M L^{-3}$)
 ρ_d = biofilm dry density ($M L^{-3}$)
 ρ_p = biofilm-coated particle effective density ($M L^{-3}$)
 ρ_l = liquid density ($M L^{-3}$)
 ρ_w = biofilm wet density ($M L^{-3}$)

Literature Cited

- Nicolella C, Van Loosdrecht MMC, Heijnen JJ. Wastewater treatment with particulate biofilm reactors. *J Biotechnol.* 2000;82:1–33.
- Patel A, Zhu J, Nakhla G. Simultaneous carbon, nitrogen and phosphorus removal from municipal wastewater in a circulating fluidized bed bioreactor. *Chemosphere.* 2006;65:1103–1112.
- Haider A, Levenspiel O. Drag coefficient and terminal velocity of spherical and non-spherical particles. *Powder Technol.* 1989;58: 63–70.
- Perry HP, Chilton CH. *Chemical Engineer's Handbook*, 5th ed. New York: McGrawHill, 1973.
- Hermanowicz SW, Ganczarczyk JJ. Some fluidization characteristics of biological beds. *Biotechnol Bioeng.* 1983;25:1321–1330.
- Mulcahy LT, Shieh WK. Fluidization and reactor biomass characteristics of the denitrification fluidized bed biofilm reactor. *Water Res.* 1987;21:451–458.
- Ro KS, Neethling JB. Biofilm density for biological fluidized beds. *Res J Water Pollut Control Fed.* 1991;63:815–818.

8. Yu H, Rittmann BE. Predicting bed expansion and phase holdups for three-phase fluidized bed reactors with and without biofilm. *Water Res.* 1997;31:2604–2616.
9. Nicolella C, Di Felice R, Rovatti M. Biomass concentration in fluidized bed biological reactors. *Water Res.* 1997;31:936–940.
10. Nicolella C, Van Loosdrecht MMC, Di Felice R, Rovatti M. Terminal settling velocity and bed-expansion characteristics of biofilm coated particles. *Biotechnol Bioeng.* 1999;62:62–70.
11. Boaventura RA, Rodrigues AE. Consecutive reactions in fluidized-bed biological reactors: modeling and experimental study of wastewater denitrification. *Chem Eng Sci.* 1988;43:2715–2728.
12. Hermanowicz SW, Cheng YW. Biological fluidized bed reactor: hydrodynamics, biomass distribution and performance. *Water Sci Technol.* 1980;22:193–202.
13. Coelho I, Boaventura R, Rodrigues A. Biofilm reactors: an experimental and modeling study of wastewater denitrification in fluidized-bed reactors of activated carbon particles. *Biotechnol Bioeng.* 1992;40:625–633.
14. Rabah FKJ, Dahab MF. Biofilm and biomass characteristics in high-performance fluidized bed biofilm reactor. *Water Res.* 2004;38:4262–4270.
15. Tsezos M, Benedek A. A method for the calculation of biological film volume in a fluidized bed biological reactor. *Water Res.* 1980;14:689–693.
16. Ngian KF, Martin WRB. Bed expansion characteristics of liquid fluidized particles with attached microbial growth. *Biotechnol. Bioeng.* 1980;22:1843–1856.
17. Karamanev DG. Equations for calculation of the terminal velocity and drag coefficient of solid spheres and gas bubbles. *Chem Eng Commun.* 1996;147:75–84.
18. Clift R, Grace JR, Weber ME. *Bubbles, Drops and Particles.* Academic Press: New York, 1978.
19. Turton R, Levenspiel O. A short note on the drag correlation for spheres. *Powder Technol.* 1986;47:83–85.
20. Ro KS, Neethling JB. Terminal settling velocity of bioparticles. *Res J Water Pollut Control Fed.* 1990;62:901–906.
21. Csikor Z, Mihaltz P, Czako L, Hollo J. New interpretation of expansion in biofilm-coated particle fluidization. *Appl Microbiol Biotechnol.* 1994;41:608–614.
22. Turan M, Ozturk I. Influence of different bioparticles on bed expansion characteristics of anaerobic fluidized bed reactors. *J Environ Sci Health.* 2001;A36:1041–1053.
23. Webb C, Black GM, Atkinson B. Liquid fluidization of highly porous particles. *Chem Eng Res Des* 1983;61:125–134.

Manuscript received Jun. 29, 2009, and revision received Dec. 9, 2009.